Journal of Chemical Crystallography
https://doi.org/10.1007/s10870-022-00946-0

ORIGINAL PAPER

Case of Charge-Assisted Hydrogen Bonding in the Crystal Structure of Sodium Laurate, Lauric Acid

Ibrahima Goudiaby[1,2] · Benoît Guillot[1] · Emmanuel Wenger[1] · Sarra Soudani[3] · Cherif ben Nasr[3] · Magatte Camara[2] · Abdoulaye Gassama[2] · Christian Jelsch[1]

Received: 31 January 2022 / Accepted: 22 April 2022
© The Author(s), under exclusive licence to Springer Science+Business Media, LLC, part of Springer Nature 2022

Abstract
Crystals of Sodium Laurate, Lauric Acid (NaLLA) were obtained and the structure was determined by single-crystal X-ray diffraction. The new crystal form is monoclinic of space group $P2_1/c$. The asymmetric unit contains two independent laurate molecules whose carboxylic/carboxylate groups are linked by a low barrier O-H…O hydrogen bond. Two lauric/laurate molecules are in a head-to-head configuration and the elongated hydrophobic chains are parallel to the long *b* axis. The carboxylic hydrogen atom was found to be disordered, bound on each of the two carboxylate groups in an unsymmetrical way. The non-symmetrical character of the hydrogen bond is related to the presence of two independent fatty acid molecules in the asymmetric unit and is in accordance with the different lengths of the four C-O bonds present in the molecular structure. The crystal structure was analyzed in terms of interactions on the Hirshfeld surface. The packing is stabilized by hydrogen bonds and O…Na ionic interactions in the hydrophilic layer and by C-H…H-C contacts in the hydrophobic layers which are the most enriched major contacts.

Keywords Fatty acid · Crystal structure · Low barrier hydrogen bond

Introduction

Higher fatty acids of the formula $C_nH_{2n-1}OOH$ are composed of long, saturated aliphatic chains with a carboxylic group at one of their extremities. Lauric acid $C_{12}H_{23}OOH$, or dodecanoic acid, occurs naturally in some vegetable oils, notably coconut oil [1, 2] and in the milk of some mammals [3]. The influence of lauric acid on human health and diet, as well as its well-known antimicrobial activity, have made this acid the subject of a large number of studies [4, 5].

There are several studies on the properties and behaviour of lauric acid or laurate salts in solution, different phases [6, 7] and as liquid crystal.

[8]. There is also interest in the solid state of lauric acid. The normal chain monocarboxylic acids with even number of carbon atoms were known to exist in three main crystalline forms which have been called A, B and C by [9], and respectively γ, β and α by [10]. The different forms can be distinguished from each other by the value of the long spacing which, for a given acid, is greatest for the γ-form and smallest for the α-form. Long chain aliphatic compounds adopt even more solid forms, with different configurations of the packing of the molecules in and between the layers [11].

Saturated carboxylic acids show polymorphism in the solid state. At least seven solid phases exist for the even members [12], called A2, Asuper, Bo, Bm, Eo, Em and C and five for the odd-numbered [13] called A', B', C', C'' and D'.

Generally, the crystal structures of these forms consist of molecules packed in bilayers containing two molecules. The carbon chains saturated are in the trans conformation (except for the B form and some triclinic forms, where the

✉ Christian Jelsch
christian.jelsch@univ-lorraine.fr

1 Université de Lorraine, CNRS, CRM2, F-54000 Nancy, France

2 Groupe Matériaux Inorganiques : Chimie Douce et Cristallographie, LCPM, Assane SECK University of Ziguinchor, Ziguinchor, Senegal

3 Laboratoire de Chimie des Matériaux, Faculté des Sciences de Bizerte, Université de Carthage, 7021 Zarzouna, Tunisia

Published online: 19 May 2022

molecules adopt a left-hand conformation), and with their carboxyl groups forming dimers through a typical R_2^2 (8) hydrogen bonding system [14]. Two types of molecular conformations of lauric acid exist in the crystal structure. One is the ordinary type, as seen in the C-form or the A_1 form belonging to the A form, while in the other one the carboxyl group is rotated about the C1-C2 bond [15].

The structures of several polymorphic crystal forms of lauric acid and laurate salts have been described. The first crystal structure reported was that of strontium laurate, in $P2_1/n$ monoclinic space group [16]. In the same year, the crystal structures of several C2/n silver fatty acids, including laurate, were analyzed and turned out to be all triclinic of space group $P\bar{1}$ [17].

The form C of lauric acid crystal structure was determined from monoclinic crystals of space group $P2_1/a$ [18]. Crystals of the γ form of lauric acid were obtained by [19] and the dimensions of the monoclinic unit cell were determined. A new crystal form (not of form A, B, nor C) of lauric acid was obtained by [20] and is triclinic. Form A_1 of lauric acid (triclinic $P\bar{1}$) was later determined by [21].

Five crystal structures of lauric acid are available in the Cambridge Structural Database (CSD-21) [22], corresponding to four polymorphs. Lomer [20, 21] deposited two copies of the triclinic $P\bar{1}$ structure. The form A crystal structure has been deposited [23] as well as the A-super form [15]. The latest crystal structure was deposited in 2009 and is monoclinic [24].

Only unit cells of crystals of laurate salts are available in the CCDC for silver, strontium and potassium (2 polymorphs) while the crystal structure of the salt with lead (II) [25] is available in the COD [26]. In the present paper, we report a new crystal structure of lauric acid containing two fatty acid molecules for one sodium cation in the asymmetric unit.

Materials and methods

Crystallization

The crystals were obtained in an attempt to co-crystallize lysine with sodium laurate. A stoichiometric quantity of lauric acid, lysine HCl and sodium hydroxide were dissolved in a minimal volume of ethyl acetate by stirring at 35 °C. All compounds were purchased from Sigma-Aldrich. The solution was at first left to cool to room temperature and then to 4 °C overnight.

Crystal data collection

A single crystal was carefully selected under a polarizing microscope in order to perform its structural analysis. X-ray diffraction data were collected on a Rigaku SuperNova diffractometer [27] at 100 K, using graphite mono-chromated Cu Kα radiation. The crystal structure was solved using a direct method with the SHELXT program [28] and initially refined by successive differential Fourier syntheses and a full-matrix least-squares procedure using the SHELXL program [29]. Crystal data and experimental parameters used for the intensity data collection are summarized in Table 1.

Crystal structure refinement

The crystal structure was then refined with software MoPro [30] using a multipolar atom model. The electron density was transferred from the ELMAM2 electron density database [31]. When using the multipolar atom model instead of the spherical one, the root mean square Fourier residual electron density diminished from 0.105 to 0.098 e $Å^{-3}$ and the $wR^2(I)$ factor from 13.3 to 10.5%. Initially the sodium cation position was modelled as an oxygen water atom which refined to an occupancy of 1.3. Therefore, a sodium cation was assigned to that position. The crystal structure has been deposited at the CSD (Deposition Number 2,143,409).

Table 1 Crystal data and structure parameters of the title compound

Chemical formula	$CH_3(CH_2)_{10}COOH$, $CH_3(CH_2)_{10}COO^-$, Na^+
MW ($g.mol^{-1}$)	422.601
Crystal system, space group	Monoclinic, $P2_1/c$
Temperature (K)	100(1)
a, *b*, *c* (Å)	35.3860 (2), 7.0683 (6), 9.8952(6)
β (°)	93.5200 (6)
V ($Å^3$) ; Z	2470.307 (6) ; 4
Data collection	
Radiation type	Cu Ka
Wavelength *λ* (Å)	1.54184
Crystal size (mm)	0.041, 0.068, 0.178
Diffractometer	Bruker SMART X2S benchtop
Absorption correction	Multi-scan (SADABS; Bruker, 2016)
T_{min}, T_{max}	0.694, 1.000
No. of measured reflections	15 823
R_{int} (%)	6.3
$sin\theta_{max}/\lambda$ ($Å^{-1}$)	0.63
Refinement	4
$wR^2[F^2 > 2\sigma(F^2)]$, $wR(F^2)$, *gof*	0.089, 0.105, 1.03
$R[F > 4\sigma(F)]$, $R(F)$	0.052, 0.073
No. of reflections	4906
No. of parameters	455
$\Delta\rho_{max}$, $\Delta\rho_{min}$, rms (e $Å^{-3}$)	0.45, -0.44, 0.098

Results and discussion

The low barrier hydrogen bond

In the NaLLA crystal structure, a single hydrogen bond between O4 and O3A atoms, is linking together the two fatty acid molecules of the asymmetric unit and displays interesting peculiarities (Fig. 1).

At first, the short O4B…O5A distance $d_{O\ldots O} = 2.452(3)$ Å obviously classifies this interaction among the strong intermolecular hydrogen bonds [32]. The O…O distance is significantly shorter than the ones found in odd and even-numbered fatty acid crystal structures. The shortest reported O…O distance is 2.54(4) Å, seen in $C_{13}H_{25}OOH$ crystal structure [11], but measured by X-ray diffraction experiments at room temperature (versus $T = 100$ K in the present study). Short ($d_{O\ldots O} < 2.65$ Å) or very short ($d_{O\ldots O} < 2.5$ Å) intermolecular O-H…O hydrogen bonds are often observed between pairs of carboxylic acids or between interacting carboxylic acids – carboxylate groups as seen in a search of the CSD version 2021. Also, O…O distances as short as 2.5 Å can be seen in intramolecular H-bond cases [33], where resonance-assisted hydrogen bonds (RAHB) are modeled against diffraction data as symmetrical, displaying a shared hydrogen atom which can be found located at equal distance from the two oxygen atoms [34].

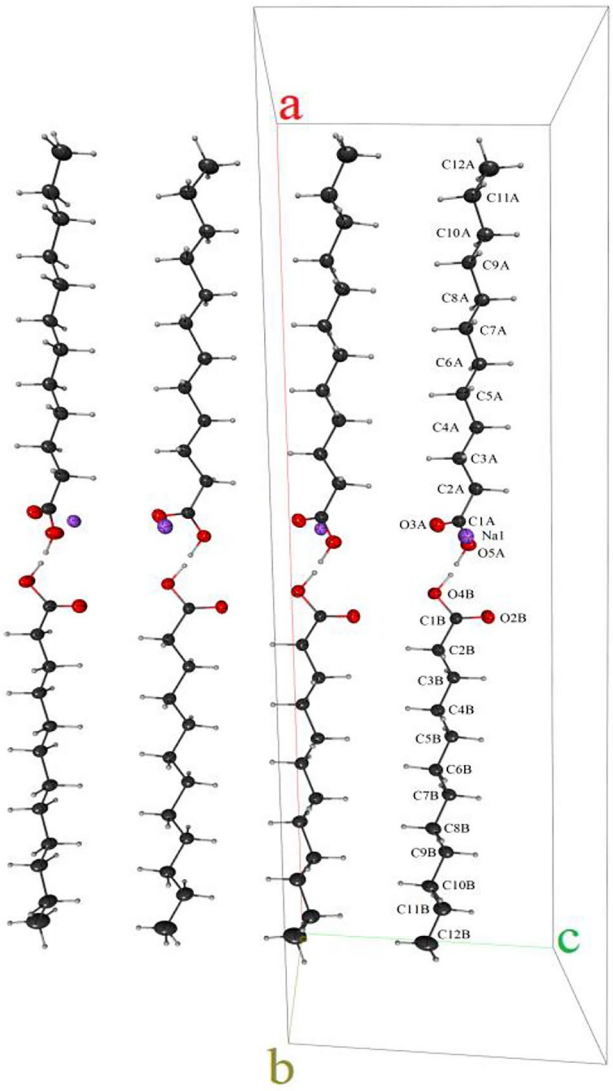

Fig. 1 Crystallographic autostereogram of four symmetry homologues in the crystal structure of the title compound. Displacement ellipsoids are drawn at the 67% probability levels. The symmetry cards are from left to right: (x, -y +½, z-3/$_2$), (x, y, z-1), (x, -y +½, z-½), (x, y, z)

The C-O bond lengths suggest a carboxylic acid character for both interacting moieties, with one short distance and one longer distance: d(C1B-O4B) = 1.306(3) Å, d(C1-O2B) = 1.219(3) Å on one side and d(C1A-O5A) = 1.300(4) Å, d(C1A-O3A) = 1.246(4) Å on the other molecule. Therefore, an H omit map was computed in the region around the O4B and O5A atoms which should bear a hydrogen atom (Fig. 2). The omit map shows an elongated density between the O4B and O5A atoms. To increase the quality of the signal, a Fourier residual map with application of a simplified noise reduction technique, inspired from Ursby & Bourgeois [35] was computed. The Fourier synthesis was performed on (Fobs – Fcalc) * R,where $R = |F\text{obs} - F\text{calc}| / [\ |F\text{obs} - F\text{calc}| + \text{Sigma}(F\text{obs}) * gof\ ]$

The R coefficient depends on the structure factor uncertainty σ(Fobs) multiplied by the goodness of fit (gof); it attenuates Fobs – Fcalc differences which are small compared to the estimated error. The resulting omit map with noise reduction shows two residual peaks (Fig. 3). The main residual peak map appears to be related to a hydrogen atom bound to the O4B atom which shows the longest C-O distance. The smallest peak corresponds to a hydrogen atom bound to O5A. The sum of occupancies of the two hydrogen atoms was constrained to unity and the occupancy values refined to q(HOB) = 0.66(8) and q(HOA) = 0.34(8). The 0.006 Å difference between the two longer C-O bond lengths is however only around two sigmas of their uncertainty (ca. 0.003 Å).

This disordered hydrogen atom HOB/HOA suggests the presence of an asymmetric double-well low-barrier hydrogen bond (LBHB) between the two independent organic molecules in the crystal structure of Sodium Laurate / Lauric Acid.

Standard hydrogen bonds are longer (e.g. 2.8 Å for an O···O H-bond), and the hydrogen atom is clearly bound

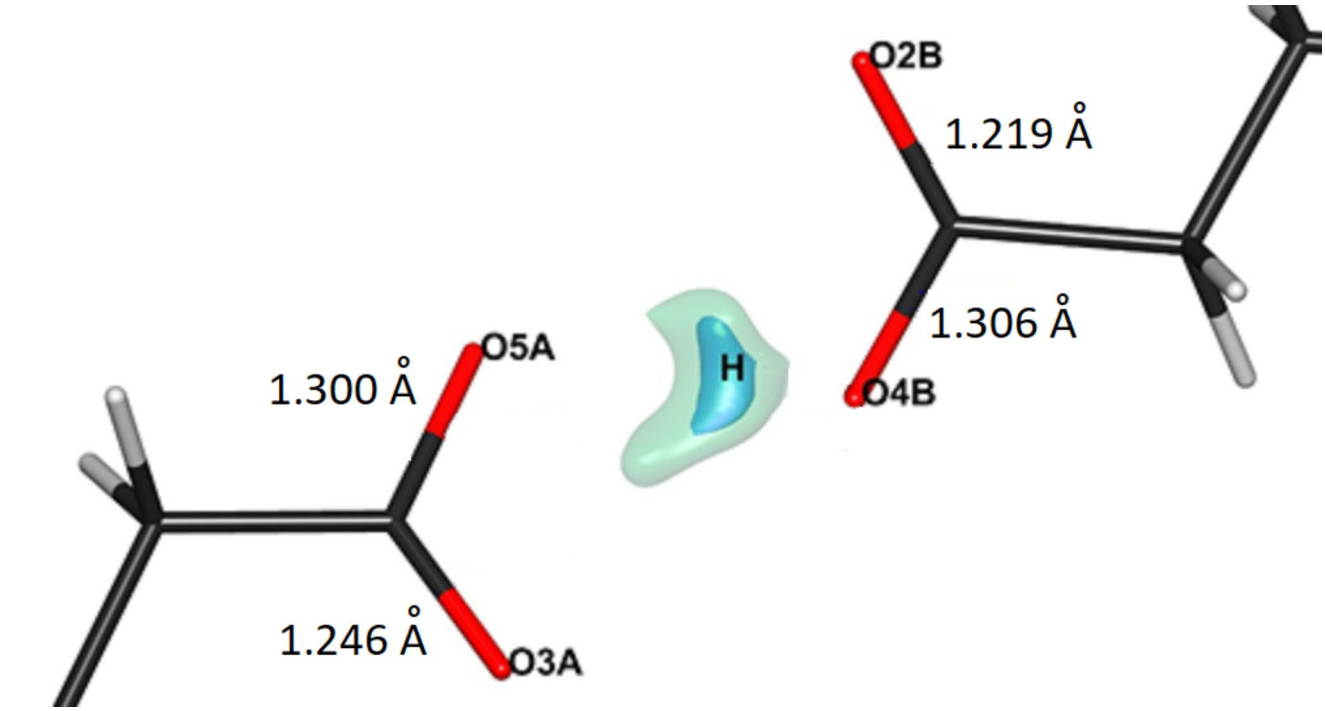

Fig. 2 Fourier residual omit H map in the O4B….O5A region. Contour levels 0.4 (blue) and 0.5 (green) e.Å^{-3}

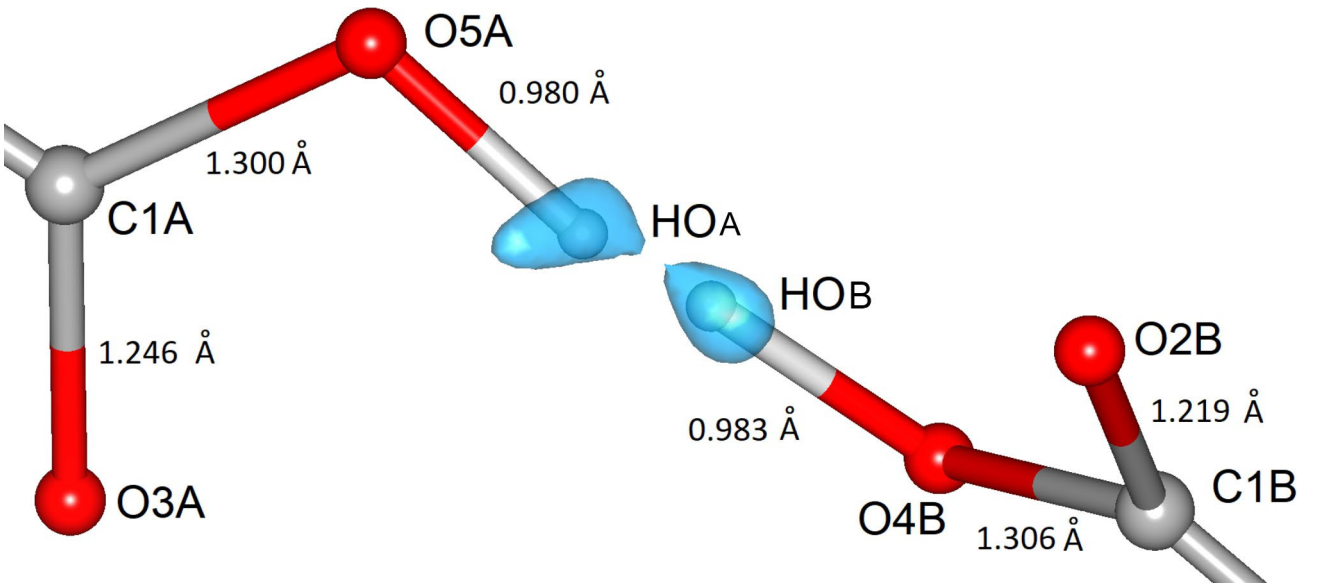

Fig. 3 The omit H map in blue at contour level at 0.27 e.Å^{-3}. The Fourier residual map using terms (*F*obs – *F*calc) * *R* was computed by applying a noise reduction technique

to one of the oxygen atoms. When the pKa of the interacting moieties is closely matched, a LBHB becomes possible at short distances (~2.55 Å). When the distance further decreases (<2.29 Å) the bond is characterized as a single-well or short-strong hydrogen bond [36]. The present crystal structure, with an O…O distance of 2.452(3) Å, corresponds to an unsymmetrical double well, corroborated by the interaction between two independent molecules in the crystal asymmetric unit.

The positive charge of the Na^+ ion is compensated by a formal negative charge of -1e shared by the pair of carboxylate/carboxylic acid groups. The O4B-HOB…O3A and O4B…HOA-O3A interactions fall therefore within the

negative-charge assisted hydrogen bond ([COO-H-COO]$^-$ CAHB) category.

The typical C-O$^-$ distance is 1.25(2) Å in carboxylate groups while in the carboxylic acid group, the bond lengths are *d*(C=O)=1.21(1) Å and *d*(C-O)=1.31(2)Å [37]. The C1B-O4B and C1A-O5A bonds, involving the oxygen atoms bound to the disordered hydrogen atom, have lengths very slightly smaller than the typical C-O distance in carboxylic acids. The two other C-O distances are intermediate between the C=O distance in carboxylic acids and the carboxylate C-O$^-$ distance. The C1B-O2B distance of 1.219(3) Å on the carboxylic group with two thirds protonation is close to C=O distance in carboxylic acids while the C1A-O3A distance 1.246(4) Å) (on COOH group with one third protonation) is closer to the carboxylate C-O$^-$ bond length.

Disordered hydrogen atom within a hydrogen bond has been observed in the recent crystal structure of 4-[(morpholin-4-yl)-carbothioyl]benzoic acid [38]. It reveals the case of a COOH…HOOC double hydrogen bond between two carboxylic acids related by an inversion centre, where the H-O hydrogen is shared between the oxygen atoms, the two C-O distances 1.266 and 1.268 Å being nearly similar.

In the crystal structure of potassium hydrogen acetylenedicarboxylate [39, 40] a hydrogen atom is found between two oxygen atom of two HOOC-C_2H_2-COO$^-$ moieties. This situation resembles that of the NaLLA crystal structure, except that it has single H atom which is located on the 2-fold symmetry axis relating the two oxygen atoms.

Table 2 Selection of bond lengths (Å) and bond angles (°) for non-H atoms with uncertainty of values given in parentheses. Symmetry operators : (i) -x+1 ; y+½ ; -z+3/2 (ii) -x+1 ; -y+1 ; -z+1.

atoms	distance	atoms	distance / angle
Na1 O4B (i)	2.322(2)	Na1 O2B (ii)	2.322(2)
Na1 O3A (i)	2.406(2)	Na1 O5A (ii)	2.386(2)
O3A C1A	1.246(4)	O2B C1B O4B	123.5(2)
O5A C1A	1.300(4)	O2B C1B C2B	121.9(2)
C2A C1A	1.514(4)	O4B C1B C2B	114.5(2)
O2B C1B	1.219(3)	O5A C1A O3A	122.9(2)
O4B C1B	1.306(3)	O5A C1A C2A	114.7(2)
C2B C1B	1.511(4)	O3A C1A C2A	122.3(2)

Crystal structure description

X-ray analysis of the crystal structure reveals that the title compound crystallizes in the monoclinic space group $P2_1/c$ with Z=4 (Table 1). Its molecular structure is shown in Fig. 1 and selected interatomic distances and angles are listed in Table 2. Table 3 lists the hydrogen bonds observed in the crystal structure. The asymmetric unit of this complex, shown in Fig. 1 consists of a sodium Na^+ cation and two interacting fatty acid molecules sharing a single negative formal charge.

The packing of the NaLLA crystal structure displays van der Waals dispersive (hydrophobic) contacts between hydrogen atoms of almost perfectly parallel *n*-alkyl chains, as it is systematically observed in saturated fatty acids crystal structures. The asymmetric low barrier hydrogen bond involves the carboxylic heads of the two laurate / lauric acid molecules. The Na^+…Oxygen electrostatic interactions and two weak C-H…O hydrogen bonds complete the interaction network.

Further comparisons of the packing observed in the present crystal structure and the ones typically seen in saturated fatty acids crystal structure reveal however striking differences.

At first, in C_nOOH, *n* odd- and even-numbered fatty acids crystal structures [11, 24], molecules are related by inversion centers found among symmetry elements of their space groups (very often monoclinic $P2_1/a$ with $Z=4$, $A2/a$ with $Z=8$ or $P\bar{1}$ with $Z=2$), with one molecule per asymmetric unit. Therefore, the conformations of interacting carboxylic groups in these centrosymmetric dimers are similar: they are either *cis* or *trans* with C-C-C=O torsion angle very close to 0° or 180°, respectively. Even-numbered saturated fatty acids (as is C12 lauric acid) noteworthily present systematic *cis* conformations with C-C-C=O torsion angles not exceeding 4°. In the present NaLLA crystal structure, this conformation is significantly distorted, with a *cis* conformation and C-C-C=O dihedral angles of 12.1° and 31.8° for the two molecules in the asymmetric unit. Consequently here, none of the two carboxyl groups are coplanar with the hydrocarbon chain of the molecule they belong to.

Furthermore, an interaction between two carboxylic groups where the two COOH groups related by inversion symmetry are facing each other in a $R_2^2(8)$ pattern, with two identical C-O-H…O=C hydrogen bonds is often seen in

Table 3 Geometric details of hydrogen bonds (Å, °) (D-donor; A-acceptor; H-hydrogen) of the title compound and symmetry code of acceptor atom

Interaction D-H…A	*d*(D—H)	*d*(H···A)	*d*(D···A)	∠D—H···A	symmetry
O4*B*—H*OB*···O5*A*	1.02	1.48	2.452 (3)	169	*x*, *y*, *z*
O5*A*—H*OA*···O4*B*	1.02	1.48	2.452 (3)	169	*x*, *y*, *z*
C2*B*—H2*D*···O2*B*^{i}	1.09	2.62	3.489 (3)	136	*x*, −*y*+ ½, *z*−½
C3*A*—H3*B*···O2*B*^{ii}	1.09	2.50	3.394 (3)	138	−*x*+1,*y*+½,−*z*+3/2

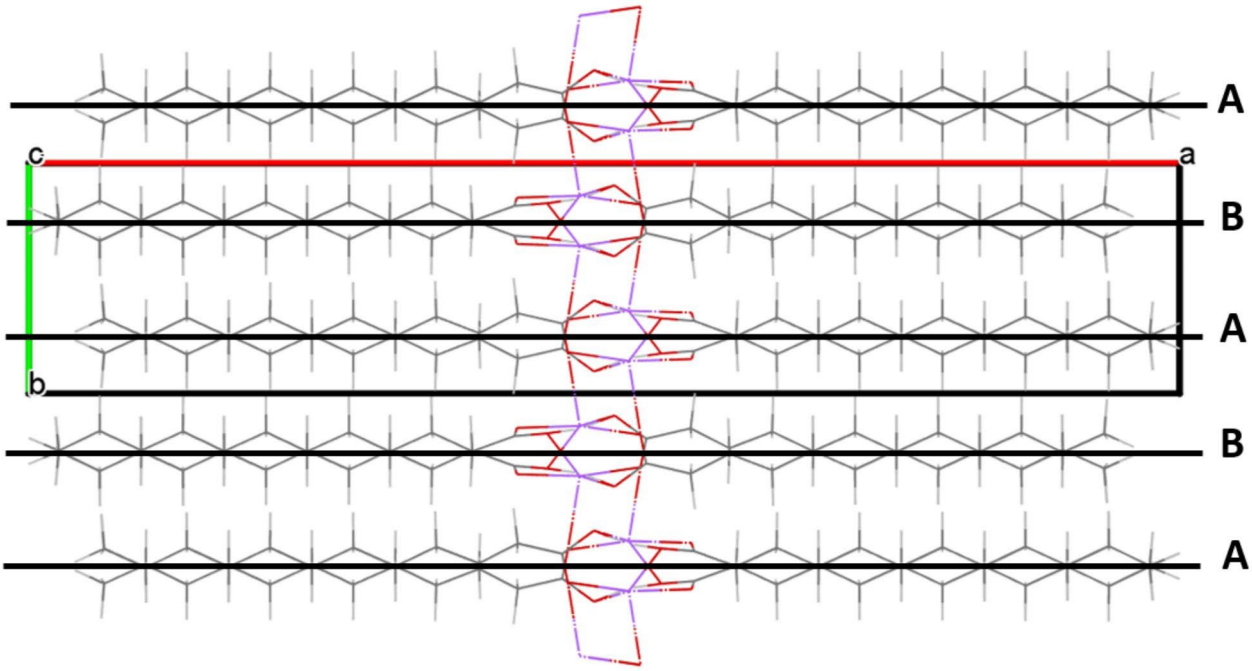

Fig. 4 View along the **c** axis of the bidimensional supramolecular structure of the NaLLA crystal structure. Axes A and B show the parallelism of double chains

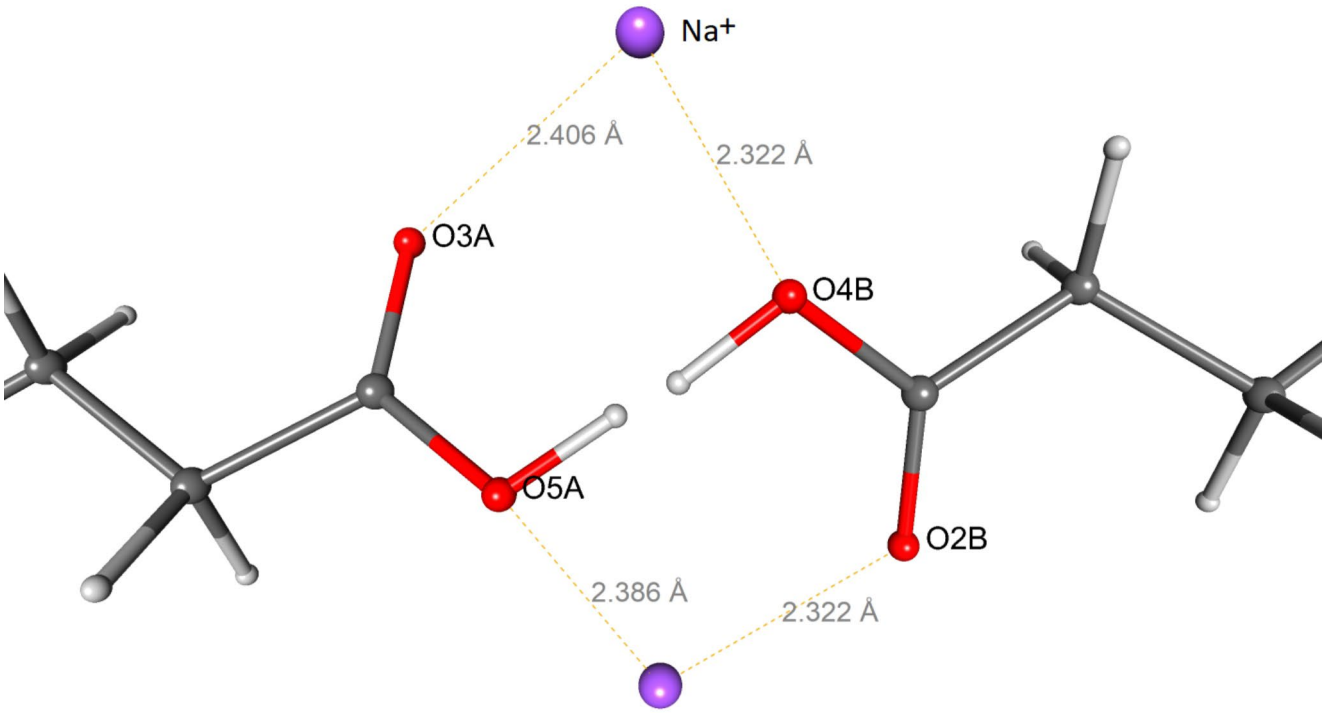

Fig. 5 View of the two closest sodium cations interacting with the oxygen atoms of the title compound

fatty acids crystal structures. Such a COOH…COOH homosynthon [41] is not observed here. Instead, the carboxylic groups are slightly rotated, forming a O-H…O hydrogen bond. These strong O-H…O hydrogen bonds, connecting opposite double chains, form layers spreading along [100] direction (Fig. 4; Table 3). Interestingly, the carboxylic oxygen atoms not involved in O-H…O hydrogen bonds, despite their strong hydrogen bond acceptor nature, only form weak C-H…O interactions with neighboring molecules (Table 3). The main interaction partners in the crystal packing of the non-protonated carboxylic oxygen atoms are the Na^+ cations. Indeed, there are four O…Na^+ interactions (2.320 Å < $d_{O...Na+}$ < 2.406 Å) between the four oxygen atoms of the asymmetric unit and two Na^+ cations located on both sides of the interacting carboxyl groups (Fig. 6).

The distortion of the usually observed *cis* conformations of the C-C-C = O groups might be attributable to these Na^+ cations present in the crystal packing. The four Na^+ ions in the unit cell are arranged around a plane perpendicular to the [100] direction roughly located at coordinate $x \sim 0.5$. The Na^+ cations are surrounded by five negatively charged oxygen atoms, three of C-O functions O3A, $O3A^{i}$ (i = 1-*x*,1-*y*,1-*z*) and $O2B^{iii}$ (iii = x,½-y,-½+z) and two corresponding to C-O-H groups, $O5A^{iii}$ (iii = (*x*,½-*y*,-½+*z*) and O4B. The Na…O distances, ranging from 2.322(3) to 2.406(3) Å (Table 2; Fig. 5), are consistent with related penta-coordinated Na complexes [42, 43]. The $Na1\cdots Na1^{i}$ and $Na1\cdots Na1^{ii}$ separations are 3.341(3) and 5.183(3) Å respectively.

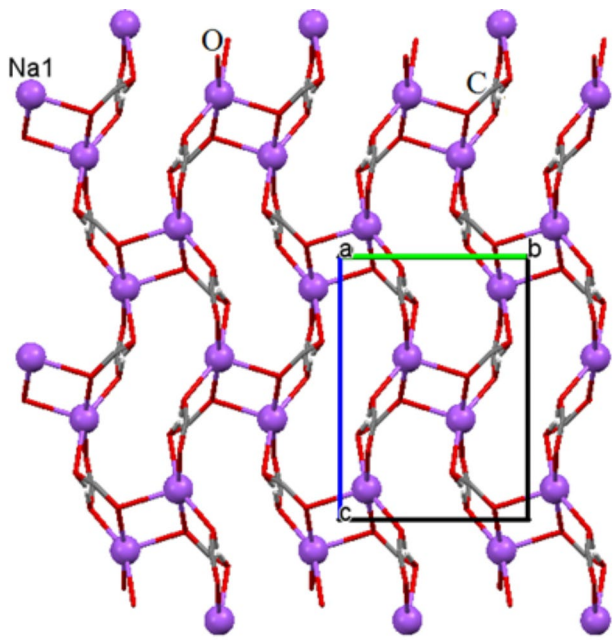

Fig. 6 Projection of a 2-D layers of sodium cations in the crystal structure along the *a*-axis. The carbon chains of lauric acid and laurate molecules have been omitted for clarity

Also, it is worth noting that these distances are significantly shorter than the sum of the van der Waals radius of the oxygen atom (R_{vdw} ~1.52 Å) and of the ionic radius of the Na^+ ion (R_{Na+} ~ 1.16 Å). Hence these strong Na^+….O electrostatic attractions may induce the distorted conformations of the fatty acid heads.

Figure 4 shows clearly the respective disposition of the aliphatic hydrocarbons of lauric acid/laurate anion and of the inorganic parts in the title compound. The polymeric chains of sodium cations, which are connected by oxygen bridges around the $x = n + ½$ planes (Fig. 5), form 2-D layers parallel to the *bc* plane.

The adjacent lauric acid/laurate molecules form face-to-face arrangements in the crystal packing (Fig. 1). These chains, which are almost parallel along the *a*-axis direction, form zig-zag planes of adjacent molecules which are perpendicular to one another (Fig. 7) [24].

Hirshfeld surface analysis

The Hirshfeld surface is representative of the region in space where molecules come into contact. In the Hirshfeld surface analysis, the disordered H atom was placed on the most occupied position. The Hirshfeld representation of the Na^+ cation, the neutral organic molecule ($C_{12}H_{24}O_2$), and the organic anion $(C_{12}H_{23}O_2)^-$ of the asymmetric unit highlights intermolecular interactions between the alkyl chains in the crystal structure (Fig. 8).

The 2D fingerprint plots of the Hirshfeld surface allows to highlight the atoms participating in contacts (Fig. 9). The graph shown in Fig. 9a. represents the H…O/O…H contacts. It is characterized by two symmetrical spikes at short distance $d_i + d_e$ ~1.6 Å. These spikes are characteristic of the strong O-H…O hydrogen bond present in the crystal structure, but there are also C-H…O contacts at longer distance. The graph in Fig. 9e representing H…H contacts is characterized by an end pointing towards the origin along the diagonal corresponding to $d_i = d_i$ ~ 1.2 Å. These are C-H…H-C contacts representing 70.8% of intermolecular contacts (Table 4), due to the parallel arrangement of the fatty acids alkyl chains, and the contact between terminal methyl groups of adjacent molecules along the [100] direction. The 2D fingerprint decomposition also shows other contacts: O…Na (10.8%) which is the second major contact and C…H-C which is in third position at 8.3%.

The contacts enrichment [46], derived from the Hirshfeld surface analysis, is computed from the ratio between the actual contact surface C_{xy} in the crystal structure and the R_{xy} (random) contact computed as if all types of contacts had the same probability to form. The equiprobable contact surfaces R_{xy} are computed from the product of probabilities *S*x and *S*y which correspond to the proportions of chemical species

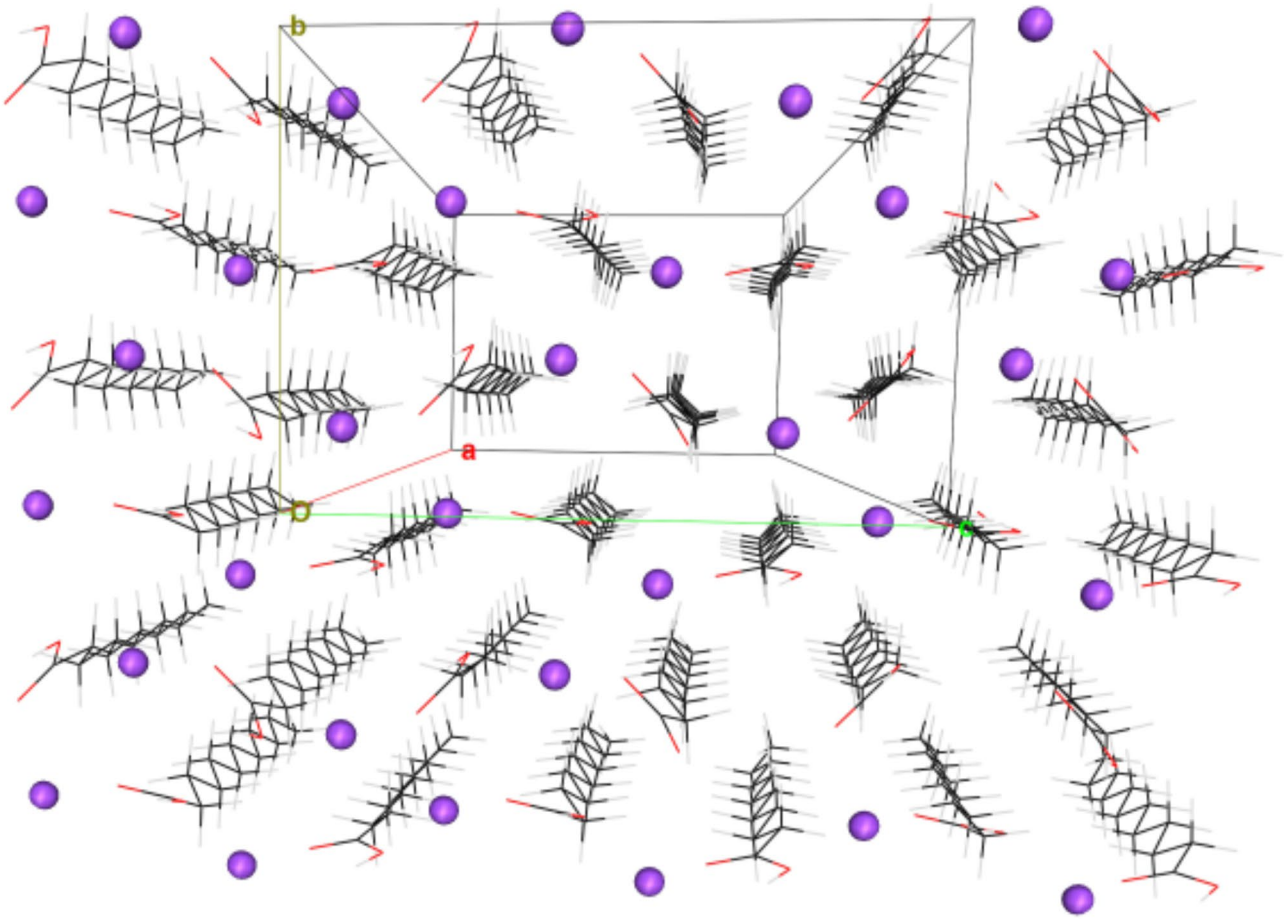

Fig. 7 Crystallographic autostereogram of a layer of NaLLA molecules parallel to the (*bc*) plane carbon: black, hydrogen: grey, oxygen: red and sodium: purple. The view was made with MoProViewer [44]

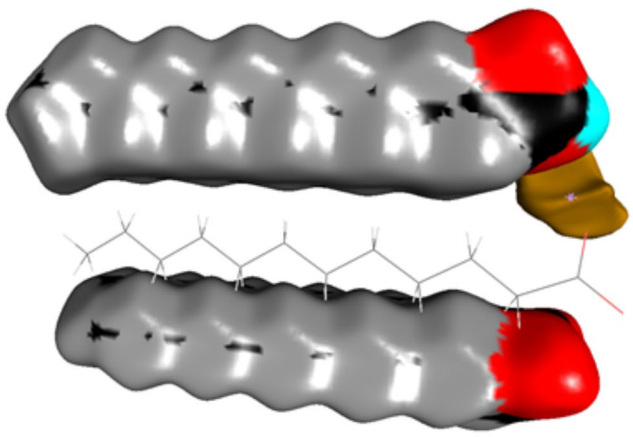

Fig. 8 Hirshfeld Surface around the lauric acid, the laurate and Na^+ moieties of the asymmetric unit. The surface is colored according to the inner chemical type: hydrogen H-C: grey, hydrogen H-O: blue, carbon: black, oxygen: red)

X and Y on the Hirshfeld surface. The contact enrichment ratio (E_{xy}) is a powerful tool to deduce which types of contacts are favoured or disfavoured in the crystal packing. An enrichment ratio E_{xy} larger than unity for a given pair of chemical species X…Y indicates that these contacts are over-represented. The contact types C_{xy} and their enrichment were computed with the MoProViewer program [45] and are shown in Table 4. For instance, the H-C hydrogen occupies 77.7% of the surface, yielding $R_{H-C,H-C} = S_{H-C}{}^2 =$ 60.4% and an enrichment $E_{H-C,H-C} = C_{H-C,H-C} / R_{H-C,H-C}$ = 70.8 / 60.4 = 1.19.

More than three quarters of the surface area is generated by H atoms. The O…Na electrostatic interactions and the O…H-O hydrogen bonds are the two strongly enriched contacts ($E_{O,H-O} > 8.3$) and constitute the two strong electrostatic interactions stabilizing the crystal packing. The large C-H…H-C contact surface between hydrophobic parts of lauric molecules is slightly over-represented at $E_{H-C,H-C} =$ 1.19. Globally the hydrophilic and hydrophobic contacts are

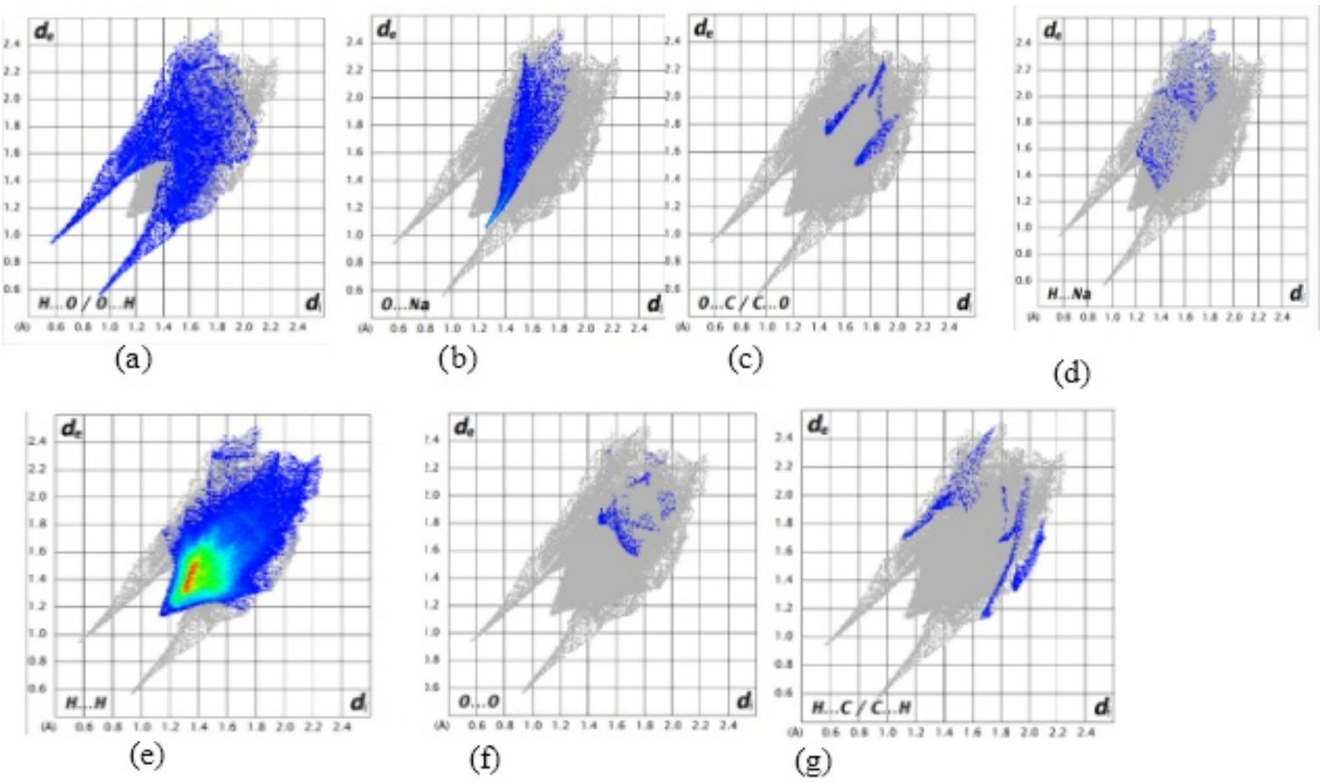

Fig. 9 Fingerprint plots in (d_i,d_e) of the main contacts on the Hirshfeld surface. The graphs were obtain with CrystalExplorer17 program [45]

enriched by 5.26 and 1.13 coefficients, respectively. Conversely the cross contacts are strongly under-represented at $E = 0.28$, in accordance with the presence of hydrophobic and hydrophilic layers in the crystal packing.

Atomic thermal motion

Using transferred multipolar pseudoatoms in a crystal structure refinement at subatomic resolution allows better estimation of atomic anisotropic thermal displacement parameters [31]. In the present NaLLA crystal structure, equivalent atomic B factors give insight to the dynamic properties of lauric acid bilayers. The two molecules in the asymmetric unit display similar dynamic behavior, with average equivalent B factors for non-H atoms of 1.6(4) Å^2 and 1.7(3) Å^2. Atomic thermal displacements within each molecule vary in similar ways along the fatty acid chain (Fig. 10). Highest B factors are found at the extremity of the fatty acids, for atoms of the terminal methyl groups: B(C12A) = 2.20 Å^2 and B(C12B) = 2.86 Å^2. The lowest atomic thermal factors, ranging from 1.36 to 1.52 Å^2, are found for C4 to C9 atoms located in the middle of the fatty acid molecules. These groups are involved in tight packing of parallel alkyl chains, where numerous H…H contacts can be found.

Table 4 Nature of intermolecular contacts on the Hirshfeld surface by chemical types. The first row and first column indicate the chemical species involved in the contacts. The second row shows the atom surfaces related to the atom types that are indicated in the first row. The percentage of actual contact types C_{xy} between chemical species is then given followed by the enrichment ratios E_{xy}. The reciprocal contacts X…Y and Y…X have been merged. The major contacts as well as the most enriched ones are highlighted in bold. The hydrophobic H-C atoms bound to carbon were distinguished from the polar Ho atom of the COOH moiety. The computation was done as if the polar hydrogen atom H-O was bound to atom O4B. The computation was done on an ensemble of lauric acid, laurate and Na^+ moieties which not in contact in order to obtain an integral surface around each moiety, as in Fig. 7. At the end of the table, the atoms were grouped in hydrophobic (H-C and C) and hydrophilic (H-O and O) atoms

atom	Na	H-O	O	H-C	C
surface S_x %	5.5	1.3	9.1	77.7	6.4
Na	0.5		C_{xy} Actual	Contacts	(%)
H-O	0.5	0.0			
O	**10.8**	1.5	0.0		
H-C	1.4	0.0	3.4	**70.8**	
C	1.5	0.2	1.0	**8.3**	0.2
Na	0.87		Enrichment	Ratio E_{xy}	
H-O	3.11	0			
O	**8.37**	**8.32**	0		
H-C	0.12	0	0.26	**1.19**	
C	1.68	1.28	1.09	0.94	0.74
	Hydrophilic	Hydrophobic		Hydrophilic/Hydrophobic	
%surface	15.9	84.1			
%contacts	2.5	70.7		26.7	
Enrichment	5.26	1.12		0.28	

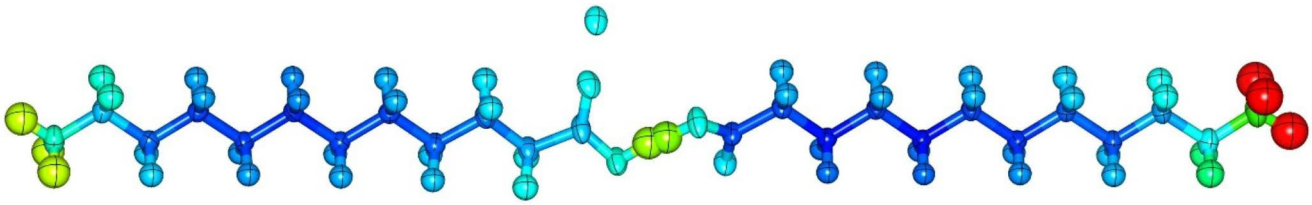

Fig. 10 NaLLA crystal structure asymmetric unit, with anisotropic thermal displacement parameters represented by ellipsoids at 75% probability. Atoms are colored according to their equivalent isotropic *B* factors: from dark blue for $B < 1.5$ Å^2 to red for $B > 4$ Å^2

Conclusion

The asymmetric unit of the new crystal contains a sodium cation and two lauric/laurate molecules in a head-to-head configuration; the elongated hydrophobic chains are parallel to the long *b* axis. The cell neutrality is obtained by a single negative formal charge shared among the two interacting carboxylate/carboxylic heads of the fatty acids through an asymmetric low barrier hydrogen bond. A low-barrier hydrogen bond (LBHB) is a special type of hydrogen bond. LBHBs can occur when the pKa of the two heteroatoms are close, which allows the hydrogen to be more equally shared between them. This hydrogen-sharing causes the formation of especially short, strong hydrogen bonds [47]. The present crystal structure of NaLLA contains formally a carboxylate group and a carboxylic acid. Therefore, the two interacting moieties (COO^-…HOOC) have identical pKas and are prone to form a LBHB, which is the case in the present crystal structure. The LBHB is found unsymmetrical with occupancy factors equal ca. to one and two thirds, in accordance with the different C-O bonds lengths found within the COO^-…HOOC moiety and with the fact that the interaction occurs between two independent molecules of the asymmetric unit.

Acknowledgements The PMD2 X-ray diffraction facility (http://crm2.univ-lorraine.fr/lab/fr/services/pmd2x) of the Institut Jean Barriol, Université de Lorraine is acknowledged for the X-ray diffraction measurements, data processing and analysis, and for providing reports for publication. I.G. thanks the Government of Senegal for scholarships and the support of Nancy ROTARY Club.

Data Availability The CIF file and hkl reflections dataset generated and analysed during the current study are available at the Cambridge Structural Database repository (Deposition Number 2,143,409), [https://www.ccdc.cam.ac.uk/]

Declarations

Conflicts of interest/Competing interests : None.

References

1. Metz J, Lassnre M (1996) Ann N Y Acad Sci 792:82–90
2. Afig MA, Rahman RA, Man YC, Al-Kahtani HA, Mansor TST (2013) Int. Food Res. J., 20:2035
3. German BJ (2008) Sci Aliments 28:176–186
4. Kavitha G, Vijayarohini P, Swamidoss CMA (2020) Mater Today-Proc., 33:2782–2791
5. Dayrit Fabian M (2015) J Am Oil Chem Soc 92:1–15
6. Li YL, Wang S, Zhang X, Chen YM, Ning JN, Liu GF, Zhang GQ (2011) Mater Sci Forum 675:227–230
7. Godquin-Giroud AM, Marchon JC, Guillon D, Skoulios A (1984) J Phys Lett 45:681–684
8. Matveeva AG, Yurtov EV, Prokopova LA (2012) Theor Found Chem Eng 46:395–400
9. Piper SH, Malkin T, Austin HE (1926) J Chem Soc 129:2310–2318
10. Thiband J, Dupré LTF (1930) C R Acad Sci Paris 191:200
11. Gbabode G, Negrier P, Mondieig D, Moreno Calvo E, Calvet T, Cuevas-Diarte M, À (2007) Chem Eur J 11:3150–3159
12. Moreno E, Cordobilla R, Calvet T, Cuevas-Diarte MA, Gbabode G, Negrier P, Oonk HA (2007) New J Chem 31:947–957
13. Gbabode G, Negrier P, Mondieig D, Moreno E, Calvet T, Cuevas-Diarte M (2009) J Alloys Compd 469:539–551
14. Bernstein J, Davis RE, Shimoni L, Chang NL (1995) Angew Chem Int Ed 34:1555–1573
15. Goto M, Asada E (1978) Bull Chem Soc Jap 51:70–74
16. Morley WM, Vand V (1949) Nature 163:285–285
17. Vand V, Aitken A, Campbell RK (1949) Acta Crystallogr 2:398–403
18. Vand V, Morley WM, Lomer TR (1951) Acta Crystallogr 4:324–329
19. Lomer TR (1955) Nature 176:653–654
20. Lomer TR, Spanswick RM (1961) Acta Crystallogr 14:312–313
21. Lomer TR (1963) Acta Crystallogr 16:984–988
22. Groom CR, Bruno IJ, Lightfoot MP, Ward SC (2016) Acta Crystallogr B: Struct Sci Cryst Eng 72:171–179
23. Von Sydow E (1956) Arkiv Kemi 9:231
24. Moreno–Calvo E, Gbabode G, Cordobilla R, Calvet T, Cuevas–Diarte MA, Negrier P, Mondieig D (2009) Chem Eur J 15:13141–13149
25. Martínez-Casado FJ, Ramos-Riesco M, Rodríguez-Cheda JA, Redondo-Yélamos MI, Garrido L, Fernández-Martínez A, Poulain A (2017) Phys Chem Chem Phys 19:17009–17018
26. Gražulis S, Chateigner D, Downs RT, Yokochi AF, T, Quirós M, Lutterotti L, Le Bail A (2009) J Appl Crystallogr 42:726–729

27. Rigaku Oxford Diffraction. (2019) CrysAlis PRO Software System, version 1.171.40.67a; Rigaku Corporation: Oxford, UK
28. Sheldrick GM (2015) Acta Crystallogr A 71:3–8
29. Sheldrick GM (2015) Acta Crystallogr C Struct chem 71:3–8
30. Jelsch C, Guillot B, Lagoutte A, Lecomte C, (2005) J Appl Crystallogr 38:38–54
31. Domagała S, Fournier B, Liebschner D, Guillot B, Jelsch C (2012) Acta Crystallogr 68:337–351
32. Gilli P, Bertolasi V, Ferretti V (1993) J Am Chem Soc 116:909–915
33. Grabowski SJ (2021) Crystals 11:5
34. Madsen GKH, Iversen BB, Larsen FK, Kapon M, Reisner GM, Herbstein FH (1998) J Am Chem Soc 120:10040–10045
35. Ursby T, Bourgeois D (1997) Acta Crystallogr A53:564–575
36. Schiøtt B, Iversen BB, Madsen GKH, Larsen FK, Bruice TC (1998) Proc. Natl. Acad. Sci. 95:12799–12802.
37. D'ascenzo L, Auffinger P (2015) Acta Crystallogr B 71:164–175
38. Agnimonhan FH, Bendeif EE, Akanni LA, Gbaguidi AF, Martin E, Wenger E, Lecomte C (2020) Acta Crystallogr E: Crystallogr Commun 76:581–584
39. Leban I, Golič L, Speakman JC (1973) J Chem Soc Perkin Trans 2:703–705
40. Kojić-Prodić B, Molčanov K (2008) Acta Chim Slov 55:692–708
41. Desiraju GR (1989) J Am Chem Soc 111:8725–8726
42. Zhang B, Xie CZ, Wang XQ, Shen GQ, Shen DZ (2004) Acta Crystallogr Sect E: Struct Rep Online 60:m1293–m1295
43. Ying-Qun Y, Shao-Hua Z, Si-Ping T, Li-Xia F (2013) Chin J Struct Chem 32:63–66
44. Guillot B, Enrique E, Huder L, Jelsch C (2014) MS19. 001. Acta Crystallogr 70:C279
45. Wolff SK, Grimwood DJ, McKinnon JJ, Turner MJ, Jayatilaka D, Spackman MA (2012) *Crystal Explorer 17.5*., Université de Western Australia
46. Jelsch C, Ejsmont K, Huder L (2014) IUCr J 1:119–128
47. Gilli G, Gilli P (2000) J Mol Struct 552:1–15

Publisher's note Springer Nature remains neutral with regard to jurisdictional claims in published maps and institutional affiliations.